

## Suppression of the First Order Vortex Melting Transition by Intrinsic Pinning in $\text{YBa}_2\text{Cu}_3\text{O}_{7-\delta}$

W. K. Kwok, J. Fendrich, U. Welp, S. Fleshler, J. Downey, and G. W. Crabtree

*Materials Science Division and Science and Technology Center for Superconductivity, Argonne National Laboratory,  
Argonne, Illinois 60439*

(Received 20 July 1993)

The first order vortex melting transition in single crystal  $\text{YBa}_2\text{Cu}_3\text{O}_{7-\delta}$  is investigated for magnetic field direction close to  $\mathbf{H}\parallel\mathbf{ab}$ . For exact field alignment  $\mathbf{H}\parallel\mathbf{ab}$ , the "kink" in  $\rho(T)$  associated with the first order melting transition is replaced with a continuous resistive transition in the presence of intrinsic pinning, indicative of a second order transition with dynamic scaling exponent  $s=1.4$ . In addition, we demonstrate the abatement of the "kink" in the temperature dependence of the magnetoresistivity, associated with the first order melting transition for  $\mathbf{H}\parallel\mathbf{c}$  in the presence of only six twin boundaries.

PACS numbers: 74.60.Ge, 74.72.Bk

Recent experiments investigating the behavior of vortex dynamics in  $\text{YBa}_2\text{Cu}_3\text{O}_{7-\delta}$  have shown support for a first order phase transition from a vortex liquid state to an Abrikosov vortex lattice state in untwinned crystals [1-3] and in high quality twinned crystals [4] when the magnetic field is misaligned with respect to the twin boundary planes. These results have led to speculations of a complex phase diagram [5] which is highly sensitive to the amount and nature of disorder in this material. In  $\text{YBa}_2\text{Cu}_3\text{O}_{7-\delta}$  thin films where a high density of defects may be responsible for effective pinning and large critical currents, the vortex liquid is proposed to freeze via a second order transition into a vortex glass state [6] at a temperature significantly below the mean field critical temperature  $T_c(H)$ . If the defects are correlated as in heavy ion induced columnar defects or twin boundaries, the low temperature solid vortex state is proposed to be a Bose glass [7].

For  $\mathbf{H}\parallel\mathbf{ab}$ , there are two qualitatively new features not present for  $\mathbf{H}\parallel\mathbf{c}$  which allow novel behavior in the possible phases and phase transitions of the vortex state. First, the anisotropic penetration depth distorts the regular hexagonal vortex pattern that would occur for  $\mathbf{H}\parallel\mathbf{c}$ , and selects a preferred orientation for the distorted structure [8], effectively inducing bond orientational order in the vortex state at all temperatures. Second, intrinsic pinning [9] tends to confine the vortices to the region between the double  $\text{CuO}_2$  planes, introducing periodic pinning sites along the  $\mathbf{c}$  direction, as opposed to the random sites in the vortex or Bose glass. This periodic pinning potential opens the possibility of induced vortex density waves with translational periodicity in the  $\mathbf{c}$  direction appearing via a second order phase transition, as in the nematic to smectic transformation in liquid crystals [10]. As the temperature is lowered, this periodicity might persist, leading to a new kind of "glass" which is random in the  $\mathbf{ab}$  plane but periodic along the  $\mathbf{c}$  direction. Such periodic vortex states will substantially differ from the vortex or Bose glass states previously studied, where random disorder provides the underlying pinning structure.

In this Letter we show for the first time evidence for the suppression of the first order vortex melting transition in the presence of intrinsic pinning. For exact alignment

of the magnetic field parallel to the  $\text{Cu-O}_2$  planes where the modulation of the order parameter along the  $\mathbf{c}$  axis leads to a weak "washboard" type potential, the discontinuity at  $\rho(T_m)$  associated with the first order vortex melting transition is replaced with a continuous resistive transition with indications of a second order transition at a lower temperature  $T^*$ . The temperature dependence of the magnetoresistivity  $\rho(T, H)$  above  $T^*$  can be fitted to a scaling behavior  $\rho \sim (T - T^*)^s$  with dynamic scaling exponent  $s \sim 1.4$ . For  $\mathbf{H}\parallel\mathbf{c}$ , we demonstrate that only six twin boundaries significantly reduces the "kink" feature associated with the first order melting transition, and the observation near  $T_m$  of a characteristic S-shaped behavior in the current-voltage response in a fixed magnetic field.

A single crystal of  $\text{YBa}_2\text{Cu}_3\text{O}_{7-\delta}$  [with dimensions  $780(l) \times 480(w) \times 57(t)$   $\mu\text{m}^3$ ] was grown by the self-flux method in a gold crucible as described elsewhere [11]. The crystal was detwinned by annealing at  $\sim 450^\circ\text{C}$  under uniaxial pressure along one of its  $\mathbf{a/b}$  crystallographic axes [12], resulting in a crystal with only six twin boundaries at 45 degrees with respect to the crystal edge as observed by polarized light microscopy. The twin boundaries crossed the region between the two voltage contacts near the bottom half of the crystal. Resistivity was measured using the standard four-probe ac technique with a typical measuring current density of  $0.3 \text{ A/cm}^2$  ( $I_s = 0.1 \text{ mA}$ ) at 17 Hz applied along one of the  $\mathbf{a/b}$  directions of the crystal. The transition temperature in zero field was  $T_c$  (midpoint) = 92.68 K with a transition width of  $\Delta T_c(10\% - 90\%) < 300 \text{ mK}$ . The normal state resistivity near  $T_c$  was  $\rho(93 \text{ K}) \sim 82.3 \mu\Omega \text{ cm}$ . Voltage-current characteristics were obtained by the dc method, reversing the measuring current polarity at each current and averaging the voltage over several readings in order to minimize thermal voltage effects. Field alignment was achieved using the "cross-field" geometry, where angular resolutions of less than  $0.001^\circ$  in the field direction can be obtained at high field [13].

The inset to Fig. 1 shows the angular dependence of the resistivity in a magnetic field of 4 T rotated in the plane perpendicular to the current direction for small angles away from the  $\mathbf{ab}$  plane of the crystal. At  $T = 90.84$

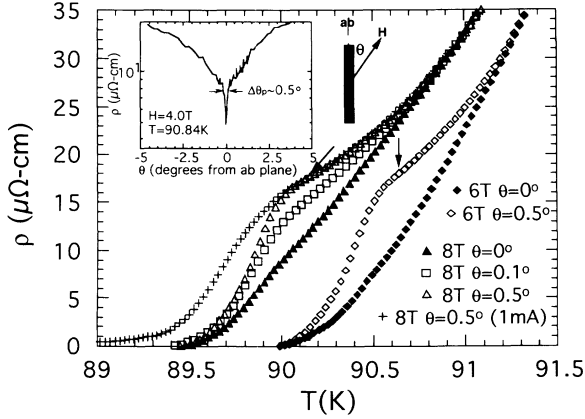


FIG. 1. Resistivity versus temperature at  $H=8$  T for  $\theta=0^\circ$ ,  $0.1^\circ$ ,  $0.5^\circ$ , and measuring currents  $I_s=0.1$  and  $1.0$  mA, and at  $H=6$  T for  $\theta=0^\circ$  and  $0.5^\circ$  and  $I_s=0.1$  mA.  $\theta$  depicts the angle between the magnetic field direction and the  $\mathbf{ab}$  plane of the crystal. The arrows mark the onset of non-Ohmic behavior. Inset: Resistivity versus angle showing the intrinsic pinning angle  $\Delta\theta_p$ .

K, we observe an extremely sharp drop in the resistivity, about  $\Delta\theta_p \sim 0.5^\circ$  wide, and centered at  $\mathbf{H}\parallel\mathbf{ab}$ . This sharp drop in resistivity has previously been reported in both twinned and untwinned crystals [13] and is the signature of intrinsic pinning of the vortices due to the layered structure of the material.

Figure 1 shows the resistive transition as a function of temperature for  $H=8$  and  $6$  T. The magnetic field orientations are  $\theta=0^\circ$  ( $\mathbf{H}\parallel\mathbf{ab}$ ),  $0.1^\circ$ , and  $0.5^\circ$  for  $H=8$  T and  $\theta=0^\circ$  and  $0.5^\circ$  for  $H=6$  T where  $\theta$  is the angle between the magnetic field direction and the  $\mathbf{ab}$  plane of the crystal. Also shown for  $H=8$  T is a curve at  $\theta=0.5^\circ$  measured with  $I_s=1.0$  mA. All other curves were obtained with a measuring current of  $I_s=0.1$  mA. Below  $T=90.8$  and  $91.25$  K for  $H=8$  and  $6$  T, respectively, a clear separation in the curves for  $\theta=0.5^\circ$  and  $0^\circ$  is observed, signaling the onset of intrinsic pinning. At lower temperatures, for  $\theta=0.5^\circ$ , a sharp kink in the resistive transition is observed for both  $H=8$  and  $6$  T near  $T_m=90.15$  and  $90.65$  K, respectively. A similar kink was reported earlier for  $\mathbf{H}\parallel\mathbf{c}$  [1] and was identified as a first order melting transition of the vortex lattice through the observation of hysteresis in  $\rho(T, H)$ . In our earlier study of the angular dependence of the magnetoresistance, we demonstrated that the kink in  $\mathbf{H}\parallel\mathbf{c}$  can be tracked closely to  $\mathbf{H}\parallel\mathbf{ab}$ , and the angular dependence of the kink can be fitted to a Lindemann criterion for melting [4,14]. More recently, hysteresis and superheating in  $\rho(T)$  [15] and hysteresis in  $\rho(H)$  [16] has been reported for  $\mathbf{H}\parallel\mathbf{ab}$  indicating that the transition represented by the kink is indeed of first order.

The curves with measuring currents  $I_s=1$  and  $0.1$  mA for  $H=8$  T and  $\theta=0.5^\circ$  show that the kink at  $T_m$  separates the *Ohmic* regime above  $T_m$  from the *non-Ohmic* regime below  $T_m$ . For  $H=8$  T, the kink disappears when the angle between the magnetic field direction and the  $\mathbf{ab}$  plane is reduced to zero. A substantial kink is

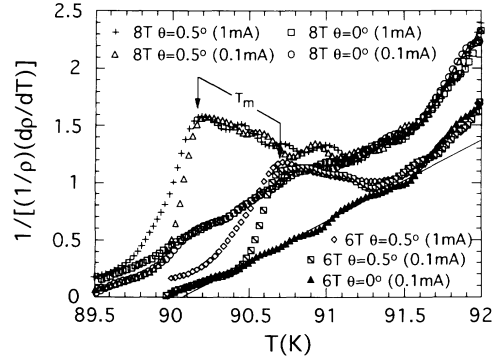


FIG. 2. Plot of  $1/[(1/\rho)(d\rho/dT)]$  vs  $T$  to determine  $T^*$  and  $s$  for  $\mathbf{H}\parallel\mathbf{ab}$ . The solid line is a fit to the data of  $\mathbf{H}=6$  T  $\parallel\mathbf{ab}$ . Also shown are data for tilted fields of  $H=8$  T at different measuring currents  $I_s=0.1$  and  $1.0$  mA.

still observed at  $\theta=0.1^\circ$ . At  $\theta=0^\circ$ , a small vestige of the kink is observable for  $H=8$  T probably due to a residual misalignment of the magnetic field. For  $H=6$  T and  $\theta=0^\circ$ , we observe a featureless smooth transition, indicating that the kink associated with the phase transition at  $T_m$  is completely suppressed. We have carefully oriented the crystal such that the magnetic field direction is at least  $40^\circ$  away from the  $\langle 110 \rangle$  direction in order to eliminate the effect of pinning from any of the six remaining twin boundaries. Thus we attribute the suppression of the melting transition  $T_m$  for  $\mathbf{H}\parallel\mathbf{ab}$  ( $\theta=0^\circ$ ) solely to intrinsic pinning by the layered structure.

Assuming that the suppression of the kink for  $\mathbf{H}\parallel\mathbf{ab}$  leads to a continuous second order transition instead of a weak first order transition, we can fit the *Ohmic* regime of the resistive tail to  $\rho \sim (T - T^*)^s$  to determine the dynamic scaling exponent  $s$  and the transition temperature  $T^*$ . Figure 2 shows a plot of  $1/[(1/\rho)(d\rho/dT)]$  vs  $T$  for  $H=8$  and  $6$  T and  $\theta=0.5^\circ$  and  $0^\circ$  with measuring currents  $I_s=1$  and  $0.1$  mA. The arrows indicate the first order vortex melting temperature  $T_m$  for  $\theta=0.5^\circ$ , below which a non-Ohmic region is clearly observed where the curves for  $I_s=1$  and  $0.1$  mA diverge. A small vestige of the kink is still noticeable for  $\theta=0^\circ$  and  $H=8$  T as demonstrated by the non-Ohmic behavior below  $T_m$ . For the  $H=6$  T and  $\theta=0^\circ$  curve, the kink is clearly suppressed and a linear behavior is observed between  $T=91.5$  and  $90.5$  K. To insure the fits contain only data with Ohmic resistivity, we performed a linear least squares fit to the data for  $H=6$  T and  $\theta=0^\circ$  from  $T=90.7$  to  $91.5$  K, where the former corresponds to  $T_m$  for the  $\theta=0.5^\circ$  geometry. We obtain a dynamic scaling exponent  $s=1.4 \pm 0.08$  from the slope of the linear fit and  $T^*=90.08$  K from the intercept, the latter corresponding within  $0.07$  K to the temperature  $T \sim 90.01$  K at which the resistivity goes to zero for  $6$  T shown in Fig. 1. The field dependence of the dynamic exponent obtained between  $H=3$  and  $8$  T is shown in the inset of Fig. 3, and found to be nearly constant in field with a value centered about  $s=1.35 \pm 0.15$ . For a transition into the

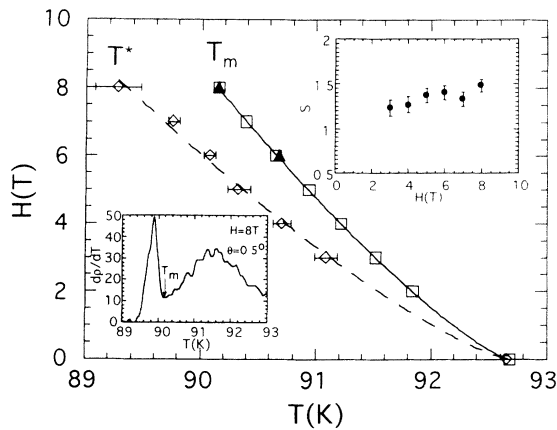


FIG. 3. Plot of  $H||ab$  versus  $T^*$  and  $T_m$ . The solid lines are a fit to  $H \sim H_0(T_c - T_m, T^*)^\alpha$ . The insets show the field dependence of  $s$  and a plot of  $dp/dT$  versus  $T$  for  $H=8$  T and  $\theta=0.5^\circ$  used to determine  $T_m$ .

vortex glass state for  $H||c$ , the dynamic exponent has been measured to be close to  $s=6.5$  ( $\nu=2.0 \pm 1$  and  $z=4.5 \pm 1.5$ ) for  $YBa_2Cu_3O_{7-\delta}$  [17,18], whereas for a columnar defect Bose glass theory,  $s=4-6$  ( $\nu' \sim 1.1-1.6$  and  $z' \sim 6.5-8.0$ ) [7]. In comparison, our obtained value of  $s$  for  $H||ab$  is much smaller and therefore may represent a different solid state than the vortex or Bose glass phase. A salient difference between the vortex and Bose glass models and intrinsic pinning is that the pin sites are randomly oriented in the glass models, but periodic along  $c$  for intrinsic pinning. The onset of intrinsic pinning provides a mechanism for inducing  $c$ -axis periodicity into the vortex structure, first as short range smectic correlations, and at  $T^*$  as a long range  $c$ -axis density wave analogous to a nematic to smectic transition in liquid crystals [10,19]. Such a transition may account for the small value of the dynamic scaling exponent which we obtain in our analysis [10,19]. Our results are in contrast with theoretical studies of interlayer vortex melting in two dimensional layered systems which generally predict that an intrinsically pinned vortex lattice cannot melt via a second order transition, [20] although others have predicted a narrow regime close to  $T_c$  where a continuous melting transition can exist [21]. The predictions for a three dimensional layered system as in  $YBa_2Cu_3O_{7-\delta}$  near  $T_c$  are yet unclear.

The temperature dependence of  $T_m$  for  $\theta=0.5^\circ$  and  $T^*$  for  $\theta=0^\circ$  is shown in Fig. 3.  $T_m$  was determined from the minima in the  $dp/dT$  vs  $T$  curves for  $\theta=0.5^\circ$  as shown in the inset to Fig. 3 for  $H=8$  T and corresponds to the onset of the resistive kink. As shown by the filled triangles in Fig. 3 for  $H=8$  and 6 T, this determination of  $T_m$  corresponds to the temperature of the onset of non-Ohmic behavior shown in Figs. 1 and 2. A power law fit to the data yields  $H(T_m) = 2.48(T_c - T_m)^{1.25}$  and  $H(T^*) = 1.70(T_c - T^*)^{1.28}$ . Although the two curves are represented on the same  $H-T$  phase diagram, we point out that the two curves represent different magnetic

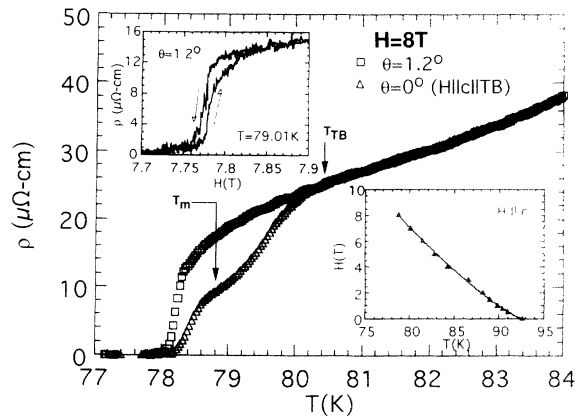


FIG. 4. Resistivity versus temperature for  $H=8$  T  $||c$  axis and tilted  $\theta=1.2^\circ$  from the  $c$  axis. The arrows show the onset of twin boundary pinning at  $T_{TB}$  and the onset of vortex lattice melting at  $T_m$ . Lower inset:  $H$  vs  $T_m$  for  $H||c$ . The solid line is a fit to a power law  $H \sim H_0(T_c - T_m)^\alpha$ . Upper inset:  $R$  vs  $H$  showing the hysteresis at  $T=79.01$  K for  $\theta=1.2^\circ$ .

field geometries:  $T_m$  represents the first order transition obtained from data for  $\theta=0.5^\circ$  and  $T^*$  the second order transition obtained from fits to the data for  $\theta=0^\circ$ .

Next we show directly that the kink in  $\rho(T)$  associated with the first order melting transition for  $H||c$  can be abated in the presence of a few twin boundaries. Figure 4 shows the resistive transition at  $H=8$  T for two different field orientations  $H||c$  and  $H$  tilted  $\theta=1.2^\circ$  from the  $c$  axis. Remarkably, for  $H||c$ , we observe a “shoulder” at  $T_{TB}=80.30$  K which signals the onset of twin boundary pinning [14], even in the presence of only six twin boundary planes. For the same curve at lower temperatures, we observe a broad kink at  $T_m$  associated with the first order phase transition from a vortex liquid into a vortex solid state [1,4,14].  $I-V$  curves for  $H||c$  (Fig. 5) show Ohmic

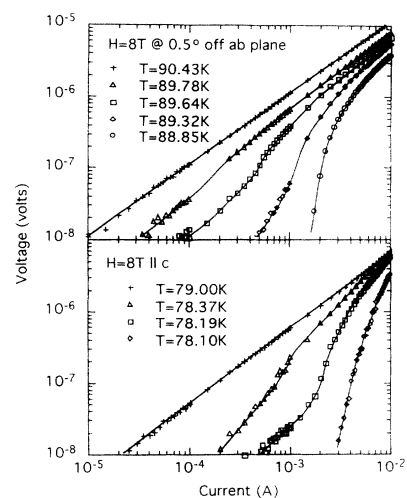


FIG. 5.  $I-V$  curves for  $H=8$  T tilted  $\theta=0.5^\circ$  off the  $ab$  plane and for  $H||c$  near the melting temperature  $T_m$ . The solid lines are a guide to the eye.

behavior above  $T_m$  and non-Ohmic behavior below. Hysteresis behavior in the field dependence of the resistivity at  $T=79.01$  K is also observed, as shown in the inset with  $\Delta H \sim 100\text{--}200$  Oe. The increasing field branch of the hysteresis curve always occurs at a higher field than the decreasing field branch. If one tilts the magnetic field by  $\theta=1.2^\circ$  so that twin boundary pinning becomes less effective, the resistive kink grows in magnitude and the shoulder due to twin boundary pinning at  $T_{TB}$  disappears. The resistive height  $\rho \sim 16 \mu\Omega \text{ cm}$  of the onset of the kink in this orientation, is exactly the same as that for the case when the magnetic field is tilted slightly off the  $\mathbf{ab}$  plane of the crystal (see Fig. 1), consistent with our earlier observation [4] that the height of the resistive melting feature is independent of the field direction. The inset to Fig. 4 shows the phase diagram of  $H$  vs  $T_m$  for  $\mathbf{H}\parallel\mathbf{c}$ . For consistency,  $T_m$  was determined from the minima in  $dp/dT$  vs  $T$  as for  $\mathbf{H}\parallel\mathbf{ab}$  above. A power law fit to the data yields  $H=0.284(T_c - T_m)^{1.26}$ . The exponent is in close agreement with the value obtained for  $\mathbf{H}\parallel\mathbf{ab}$ . The ratio of the prefactors for  $\mathbf{H}\parallel\mathbf{c}$  and  $\mathbf{H}\parallel\mathbf{ab}$  yields a mass anisotropy  $\Gamma = \sqrt{M/m} \sim 8.7$  consistent with earlier reports on single crystal  $\text{YBa}_2\text{Cu}_3\text{O}_{7-\delta}$  [22].

The  $I$ - $V$  characteristics near the kink in  $\rho(T)$  for  $H=8$  T tilted  $0.5^\circ$  from the  $\mathbf{ab}$  plane and for  $\mathbf{H}\parallel\mathbf{c}$  are shown in the top and bottom panels of Fig. 5, respectively. For magnetic fields tilted at  $0.5^\circ$  from the  $\mathbf{ab}$  plane, non-Ohmic behavior becomes apparent at  $T=89.78$  K, just below the kink temperature  $T_m=90.15$  K. Above this temperature at  $T=90.43$  K, Ohmic behavior is observed. Within the temperature width of the kink in  $\rho(T)$  for  $\theta=0.5^\circ$ ,  $89.30 \text{ K} < T < 90.15 \text{ K}$ , and S shape in the  $I$ - $V$  curve is observed. At  $T=88.85$  K and below, the S shape is replaced by a concave downward curve. A similar behavior is observed in the  $I$ - $V$  curves for  $\mathbf{H}\parallel\mathbf{c}$ . Below the onset of twin boundary pinning  $T_{TB}$  and above the melting temperature  $T_m$ , Ohmic behavior is observed as shown by the  $I$ - $V$  curve for  $T=79.00$  K. At temperatures below the kink but above the temperature where the resistivity goes to zero, an S shape appears, which is replaced by a concave downward behavior at lower temperature. Thus we propose that the S shape in the  $I$ - $V$  curve is related to the first order phase transition where the vortex liquid freezes into large domains of Abrikosov vortex lattice. The S shape separates the low current regime arising from thermally activated flux flow of the lattice from the high current linear regime arising from vortex flux flow of an unpinned lattice. At lower temperatures, the concave downward behavior suggests the formation of a true critical current associated with a glassy state. This may come about by a gradual reduction of the Abrikosov vortex lattice domain size due to quenched random disorder [23].

In summary, we have shown strong indications that the

first order melting transition is replaced by a continuous second order transition in the presence of intrinsic pinning for  $\mathbf{H}\parallel\mathbf{ab}$ . We obtain a dynamic scaling exponent of  $s \sim 1.4$ , much less than that predicted by the vortex glass or Bose glass model. In addition, we have shown directly that disorder, in the form of six twin boundaries, may reduce the kink feature in  $\rho(T)$  associated with the first order phase transition at  $T_m$  for  $\mathbf{H}\parallel\mathbf{c}$ . Furthermore, the  $I$ - $V$  characteristics near the first order transition display a characteristic S shape, which separates the unpinned vortex solid flux flow region from the thermally activated vortex solid flux flow region.

The authors thank D. R. Nelson and V. M. Vinokur for many helpful discussions. This work was supported by the U.S. Department of Energy, BES-Materials Science under Contract No. W-31-109-ENG-38 (W.K.K., J.F., S.F., J.D., G.W.C.) and the NSF-Office of Science and Technology Centers under Contract No. DMR91-20000 (U.W.) Science and Technology Center for Superconductivity.

- 
- [1] H. Safar *et al.*, Phys. Rev. Lett. **69**, 824 (1992).
  - [2] D. E. Farrell *et al.*, Phys. Rev. Lett. **67**, 1165 (1991).
  - [3] R. G. Beck *et al.*, Phys. Rev. Lett. **68**, 1594 (1992).
  - [4] W. K. Kwok *et al.*, Phys. Rev. Lett. **69**, 3370 (1992).
  - [5] H. Safar *et al.*, Phys. Rev. Lett. **70**, 3800 (1993).
  - [6] M. P. A. Fisher, Phys. Rev. Lett. **62**, 1415 (1989); D. S. Fisher *et al.*, Phys. Rev. B **43**, 130 (1991).
  - [7] D. R. Nelson and V. M. Vinokur, Phys. Rev. Lett. **68**, 2398 (1992).
  - [8] K. Takanaka, Phys. Status Solidi (b) **68**, 623 (1975); V. G. Kogan, Phys. Rev. B **24**, 1572 (1981).
  - [9] M. Tachiki and S. Takahashi, Solid State Commun. **70**, 291 (1989).
  - [10] D. R. Nelson (private communication); see Appendix A in D. R. Nelson and V. M. Vinokur, Phys. Rev. B **48**, 13060 (1993).
  - [11] D. L. Kaiser *et al.*, J. Cryst. Growth **85**, 593 (1987).
  - [12] U. Welp *et al.*, Physica (Amsterdam) **161C**, 1 (1989).
  - [13] W. K. Kwok *et al.*, Phys. Rev. Lett. **67**, 390 (1991).
  - [14] S. Fleshler *et al.*, Phys. Rev. B **47**, 14448 (1993).
  - [15] M. Charalambous *et al.*, Phys. Rev. Lett. **71**, 436 (1993).
  - [16] J. Fendrich *et al.* (unpublished).
  - [17] R. H. Koch *et al.*, Phys. Rev. Lett. **63**, 1511 (1989).
  - [18] P. L. Gammel *et al.*, Phys. Rev. Lett. **66**, 953 (1991).
  - [19] P. G. de Gennes, Solid State Commun. **10**, 753 (1972).
  - [20] L. V. Mikheev and E. B. Kolomeisky, Phys. Rev. B **43**, 10431 (1991); S. E. Korshunov and A. I. Larkin, Phys. Rev. B **46**, 6395 (1992).
  - [21] B. Horowitz, Phys. Rev. Lett. **67**, 378 (1991).
  - [22] D. E. Farrell *et al.*, Phys. Rev. Lett. **64**, 1573 (1990).
  - [23] A. I. Larkin, Zh. Eksp. Teor. Fiz. **58**, 1466 (1970) [Sov. Phys. JETP **31**, 784 (1970)].